Modeling variability of plasma conditions in the Io torus

P. A. Delamere and F. Bagenal

Laboratory for Atmosphere and Space Physics, University of Colorado, Boulder, Colorado, USA

Received 27 September 2002; revised 20 January 2003; accepted 25 February 2003; published 8 July 2003.

[1] Telescopic observations and in situ measurements of the Io plasma torus show the density, temperature and composition to vary over time, sometimes up to a factor of 2. While previous models of the physical and chemical processes in the Io plasma torus have reasonably modeled the conditions of the Voyager 1 era, their authors have not addressed the observed variability nor explored the sensitivity of torus conditions to input parameters. In this paper we present a homogeneous torus model parameterized by five variables (transport timescale, neutral source strength, ratio of oxygen to sulfur atoms in the source, fraction of superthermal electrons, temperature of these hot electrons). The model incorporates the most recent data for ionization, recombination, charge exchange and radiative energy losses for the major torus species (S, S^+, S^{++}, S^{+++}, O, O^+, O^{++}). We solve equations of conservation of mass and energy to find equilibrium conditions for a set of input parameters. We compare model plasma conditions with those observed by Voyager 1, Voyager 2 and Cassini. Furthermore, we explore the sensitivity of torus conditions to each parameter. We find that (1) torus conditions are distinctly different for the Voyager 1, 2 and Cassini eras, (2) unique torus input parameters for any given era are poorly constrained given the wide range of solution space that is consistent with the range of observed torus conditions, (3) ion composition is highly sensitive to the specification of a non-thermal electron distribution, (4) neutral O/S source ratio is highly variable with model values ranging between 1.7 for Cassini to 4.0 for Voyager conditions, (5) transport times range between 23 days for Voyager 2 to 50 days for Voyager 1 and Cassini, (6) neutral source strengths range between 7 to 30 $\times$ 10^{-4} cm^{-3} s^{-1} which corresponds to a net production of 0.4 to 1.3 tons/s for a torus volume of 1.4 $\times$ 10^{31} cm^3, or 38 R_J^3. *INDEX TERMS:* 6218 Planetology: Solar System Objects: Jovian satellites; 7837 Space Plasma Physics: Neutral particles; 0343 Atmospheric Composition and Structure: Planetary atmospheres (5405, 5407, 5409, 5704, 5705, 5707); 2102 Interplanetary Physics: Corotating streams; *KEYWORDS:* Plasma, torus, Io, variability, chemistry, Jupiter

Citation: Delamere, P. A., and F. Bagenal, Modeling variability of plasma conditions in the Io torus, *J. Geophys. Res.*, *108*(A7), 1276, doi:10.1029/2002JA009706, 2003.

1. Introduction

[2] The ionization of ~1 ton/second of neutral material from Io's atmosphere produces a dense (~2000 cm^{-3}) torus of electrons, sulfur and oxygen ions, trapped in Jupiter's strong magnetic field. Emissions from the Io plasma torus are relatively well measured both from the ground (reviewed by *Spencer and Schneider* [1996]) and from space-based UV telescopes (Figure 1, see references in caption). Particularly useful is the Cassini flyby of Jupiter (Oct 2000–April 2001) when the Ultraviolet Imaging Spectrograph (UVIS) [*Esposito et al.*, 2003] made measurements of emissions from all the major ionized species over six months [*Stewart*, 2001].

[3] Analysis of torus emissions provides estimates of density, composition, and temperatures (see review by Brown, Shemansky and Johnson [*Dessler*, 1983]). Models of the mass and energy flow through the torus provide observables (electron density and temperature, ion composition and temperature) as functions of source properties (source strength and composition) and radial transport timescale. The first ab initio calculation of torus properties from ionization of a cloud of neutrals was by *Barbosa et al.* [1983]. They showed that Coulomb collisions between a population of ions (including 20% with pick-up energies) and electrons were able to power the observed UV emissions observed by the Voyager UVS [*Broadfoot*, 1979], albeit by assuming a rather high average charge state for the ions. In the past 19 years there has been an evolution of such "neutral cloud theory" (NCT) models, adopting new atomic data as they became available [e.g., *Johnson and Strobel*, 1982; *Ziegler et al.*, 1982; *Brown et al.*, 1983; *McGrath and Johnson*, 1989] and adding electron heating [*Barbosa*, 1994; *Shemansky*, 1988], velocity distribution evolution [*Smith and Strobel*, 1985], radial transport [*Bar-*

0148-0227/03/2002JA009706$09.00

bosa, 1994; *Schreier et al.*, 1998] *Matheson and Shemansky, unpublished manuscript*, 1993, and inward diffusion to the cold torus [*Richardson and Siscoe*, 1983; *Moreno and Barbosa*, 1986; *Barbosa and Moreno*, 1988]. While these models were able to match the torus conditions typical of the Voyager era (e.g., as in the empirical model of the torus published by *Bagenal* [1994]), they made limited exploration of the sensitivity of the equilibrium conditions to variations in input parameters. In this paper we explore the temporal variability of the torus properties with a homogeneous, zero-dimensional neutral cloud model and investigate the implications for variability of Io's plasma source. Despite the limitations of the homogeneous assumption, the model allows us to explore the sensitivity of model output to variations in the input parameters.

2. Observations of Torus Composition

[4] In situ measurements of plasma properties have been made by the Voyager 1 and Galileo spacecraft [*Bagenal*, 1994; *Frank and Paterson*, 2001b; *Gurnett et al.*, 2001]. Plasma measurements provide quite accurate values of electron density, temperatures (ion and electron) and, when the flow is supersonic (inside 5.7 R_J and in the plasma sheet for Voyager 1), in situ measurements put useful constraints on ion composition [*Bagenal*, 1994]. In the core of the torus (between 5.7 and 12 R_J) where the flows are subsonic, however, the composition is only weakly constrained because the spectral peaks of the different ions merge in the energy spectrum. Analysis is further complicated by the fact that the dominant species, S^{++} and O^+, have the same mass/charge ratio. *Crary et al.* [1998] used measurements of electron density from the Plasma Wave Science instrument on Galileo [*Gurnett et al.*, 1996, 2001] to constrain analysis of the Plasma Science instrument data [*Frank et al.*, 1996; *Frank and Paterson*, 2000a, 2000b, 2001a]. *Crary et al.* [1998] found higher O^+ and O^{++} abundances than during the Voyager 1 conditions but with large uncertainties (and the S^{+++} abundance was not well constrained).

[5] The best measurements of ion composition in the torus come from simultaneous observations of emission lines from major species. The strong sulfur emission lines in the FUV have been observed with astronomical telescopes (HUT, FUSE, HST) but O^+ emissions are rarely observed [*McGrath et al.*, 1993]. *Thomas* [2001] have observed visible O^+, S^+ and S^{++} emissions simultaneously from the ground. *Lichtenberg and Thomas* [2001] have managed to observe S^{+++} with ISO but not yet simultaneously with the major ion species. The most comprehensive coverage of ion emissions are in the EUV region where ultraviolet spectrometers on the Earth-orbiting EUVE telescope and the Voyager, Galileo and Cassini spacecraft have measured torus emissions from all of the major ions.

[6] Figure 1 shows twelve observations of torus composition from UV spectral measurements and results from five torus models. The observations show a wide range in the mixing ratios of sulfur (S^+/S^{++} and S^{+++}/S^{++}) as well as the ratio of total densities of oxygen to sulfur ions. The average charge state is between 1.3 and 1.5 in all cases. Some of the variations in composition are observed with similar instruments. These data have been analyzed with the same techniques and probably reflect true temporal changes in the torus. For example, compare Astro-1 vs. Astro-2 [*Feldman et al.*, 2001] in columns 1 and 2, HST C23 vs. I27 [*Herbert et al.*, 2003] in columns 4 and 5, and EUVE 96 vs. 99 [*Herbert et al.*, 2001] in columns 10 and 11. On the other hand, there is a worrying difference between torus compositions reported from analyses of the same Voyager 1 data set by *Shemansky* [1988] and *Herbert et al.* [2001] (columns 6 and 7). It should be noted that these different analyses involve different parts of the data set, different instrument sensitivity curves, and even different atomic data. Furthermore, the sulfur mixing ratios derived from emissions in the EUV (columns 10, 11 from *Herbert et al.* [2001]) are systematically different from those derived from the FUV emissions (columns 1–5 from *Feldman et al.* [2001] and *Herbert et al.* [2003]). Thus difficulties in deriving temporal changes from different data sets are compounded by uncertainties in instrument sensitivity calibrations as well as uncertainties in UV emission rates. The concept of

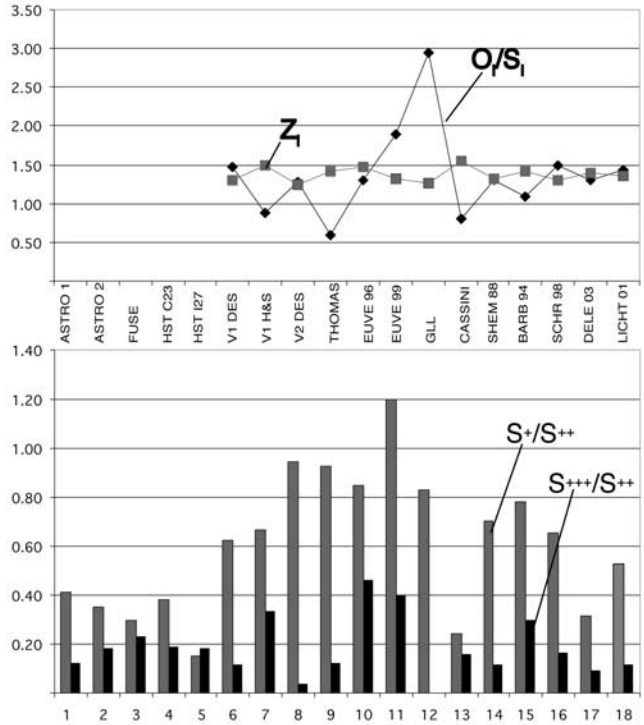

Figure 1. Composition variability: The top panel illustrates variability of average charge state (Z_i) and total ion abundance ratio (O_i/S_i), and the bottom panel shows sulfur mixing ratios for the following 17 observations and NCT models: 1–3, HUT and FUSE [*Feldman et al.*, 2001]; 4–5, HST [*Herbert et al.*, 2003]; 6, Ion composition from analysis of Voyager 1 UVS spectra by D. E. Shemansky [*Bagenal*, 1994]; 7, Analysis of Voyager 1 UVS spectra [*Herbert et al.*, 2000]; 8, Voyager 2 UVS [*Shemansky*, 1987]; 9, Ground-based spectroscopic observations taken in 1999 [*Thomas*, 2001]; 10–11, EUVE data [*Herbert et al.*, 2001]; 12, Galileo PLS data obtained Dec. 1996 [*Crary et al.*, 1998]; 13, Cassini UVIS data from Jan. 2001 [*Steffl*, 2002]; 14, NCT Model of *Shemansky* [1988]; 15, NCT Model (O/S = 3) of *Barbosa* [1994]; 16, NCT Model of *Schreier et al.* [1998]; 17, NCT Model of this paper; 18, NCT Model of *Lichtenberg* [2001].

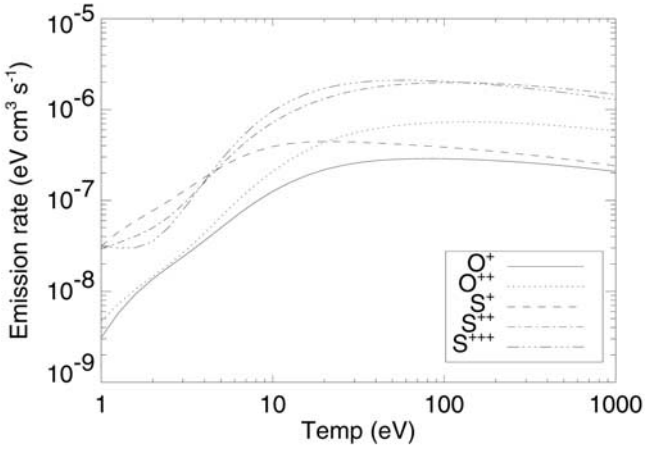

Figure 2. Emission rates by electron impact excitation, $\mathcal{R}(n_e, T_e)$, for n_e = 2000 cm^{-3}.

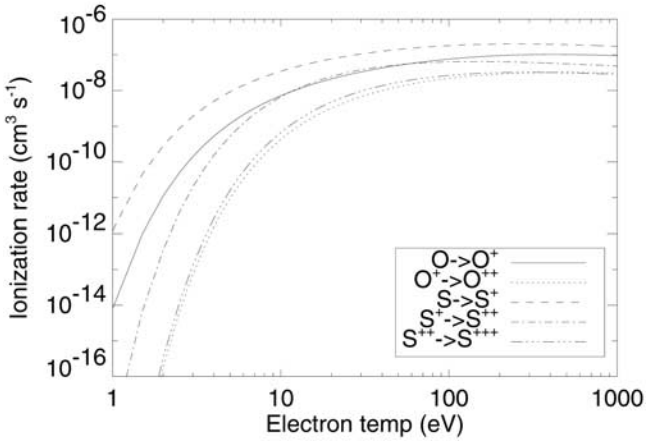

Figure 3. Ionization rates through electron impact ionization to the labeled state.

"nominal Voyager 1 conditions", Therefore should not be interpreted too rigorously.

[7] The only published ion composition for the Voyager 2 epoch is in *Shemansky* [1987] (column 8) which reports lower average charge state for the sulfur ions and a slightly higher oxygen ion fraction than during the Voyager 1 epoch. The Cassini UVIS offers some optimism since it is a consistent data set spanning the ultraviolet spectrum from FUV to EUV (561–1912 Å), with higher spectral resolution (3 Å) gathered over six months [*Stewart*, 2001]. A. Steffl (maunuscript in preparation, 2002) reports an ion composition derived from Cassini UVIS data from January 2001 in which the sulfur ions have a higher ionization state than in the Voyager epoch and the oxygen/sulfur ratio is lower.

[8] The earlier model results shown in Figure 1 were derived to match the Voyager 1 conditions [*Shemansky*, 1988; *Barbosa*, 1994; *Schreier et al.*, 1998]. The *Lichtenberg and Thomas* [2001] model was matched to a combination of ground-based and Voyager conditions. Below we discuss these models in comparison with the model presented in this paper.

3. Model

[9] Using the latest atomic data, a preliminary local (zero-dimensional) neutral cloud theory (NCT) model has been developed for the purpose of investigating the sensitivity of torus composition to the following parameters: neutral source rate ($\mathcal{S}_n$), O/S source ratio (O/S), transport loss (τ), hot electron fraction (f_{eh}), and hot electron temperature. Note that the plasma density is not constrained to a fixed value but is an output of the model. The model is based largely upon several earlier NCT models [*Shemansky*, 1988; *Barbosa*, 1994; *Schreier et al.*, 1998; *Lichtenberg and Thomas*, 2001], but uses the latest CHIANTI atomic physics database for computing radiative loss [*Dere et al.*, 1997] (Figure 2). CHIANTI is a database containing transition wavelengths, level information, oscillator strengths, and collision strengths for all ion species with $Z \leq 26$. The database is a compilation of the latest experimental and theoretical values and is updated regularly. Charge exchange rates are based on those reported by *McGrath and Johnson* [1989] for ion velocities typical of 6 R_J. Ionization rates (Figure 3) are from *Voronov* [1997]. Note that there have been ~2× variations in the ionization rates of S to S^+ since *Shemansky* [1988] (Figure 4). We also note that the ionization rates below the sulfur ionization potential (10.36 eV) are determined by convolving a Maxwellian electron energy distribution with a limited number of measured cross sections above the ionization potential. Therefore the ionization rates at the thermal electron temperature (~5 eV) are subject to considerable uncertainty. Recombination rates are from *Mazzotta et al.* [1998], *Shull and Steenberg* [1982], and *Pequignot et al.* [1991] which we have adapted from *Lichtenberg and Thomas* [2001].

[10] In this preliminary study we take a local zero-dimensional approach where we treat the transport as a (parameterized) loss rate. Radial transport rates drop abruptly inside Io's orbit, so outward transport of plasma from inside 5.7 R_J can be neglected as a source. Our main goal is to explore possible torus properties beyond 6 R_J under diffusive radial transport rather than small-scale spatial structure <6 R_J. While we recognize that the cloud of neutrals

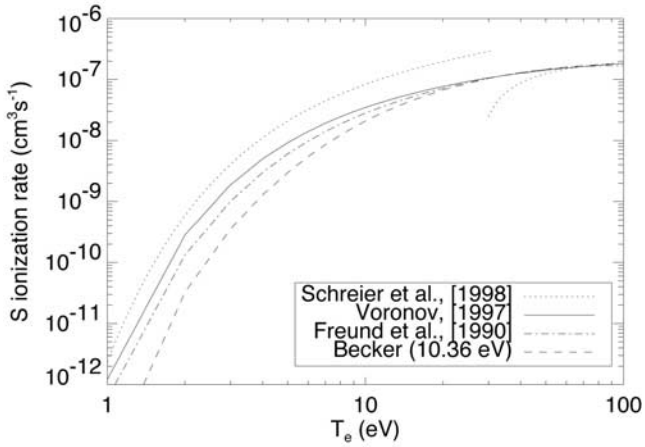

Figure 4. Variation in the ionization rates of S to S^+ as a function of temperature of a Maxwellian electron distribution found in the literature. We adopted the *Voronov* [1997] rates.

emanating from Io has complex three-dimensional structure [*Smyth*, 1992], we model a homogeneous source in order to concentrate on torus chemistry. However, the longitudinal structure of the source region can be largely ignored since transport and chemistry timescales (days) are much larger than Io's system III orbital period (hours).

3.1. Governing Equations

[11] The primary sources of mass and energy are ionization and charge exchange reactions involving neutral gas. Charge exchange reactions determine the allocation of energy among the ion species and their respective ionization states. Charge exchange reactions involving neutrals also contribute significantly to the energy budget due to the pickup energy of plasma into the corotating plasma torus. Following *Barbosa et al.* [1983], the basic equations for mass and energy for species, α, are

$$\frac{\partial n_\alpha}{\partial t} = \mathcal{S}_m - \mathcal{L}_m \tag{1}$$

$$\frac{\partial\left(\frac{3}{2} n_\alpha T_\alpha\right)}{\partial t} = \mathcal{S}_\mathcal{E} - \mathcal{L}_\mathcal{E} \tag{2}$$

(From here forward, the factor of 3/2 will be dropped and thus we are solving for temperature balance rather than energy balance.)

[12] The source rate for the density of each ion species, n_α, is

$$\mathcal{S}_m = I_{\alpha_-} n_{\alpha_-} n_e + I^h_{\alpha_-} n_{\alpha_-} n_{e,hot} + R_{\alpha_+} n_{\alpha_+} n_e + \sum_{\gamma,\beta} k_{\gamma,\beta} n_\gamma n_\beta \tag{3}$$

where I and I^h are the electron impact ionization rates for the thermal and hot electron populations respectively, R is the recombination rate, α_- and α_+ are the lower and higher ionization states of species α, and $k_{\gamma,\beta}$ symbolically represents all charge exchange reaction rates between ions and neutrals which produce species α given in Table 1.

[13] The loss rate for the density of each species, n_α, is

$$\mathcal{L}_m = I_\alpha n_\alpha n_e + I^h_\alpha n_\alpha n_{e,hot} + R_\alpha n_\alpha n_e + \sum_\beta k_{\alpha,\beta} n_\alpha n_\beta + \frac{n_\alpha}{\tau} \tag{4}$$

where τ is the transport timescale.

[14] The energy input rate for a given species is

$$\mathcal{S}_\mathcal{E} = I_{\alpha_-} n_e n_{\alpha_-} T_{\alpha_-} + I^h_{\alpha_-} n_{e,hot} n_{\alpha_-} T_{\alpha_-} + R_{\alpha_+} n_{\alpha_+} n_e T_{\alpha_+} + \sum_{\gamma,\beta} k_{\gamma,\beta} n_\gamma n_\beta T_\beta + \sum_{\beta=i,e} \nu^{\alpha/\beta} n_\alpha \left(T_\beta - T_\alpha\right) \tag{5}$$

where $\nu^{\alpha/\beta}$ is the thermal equilibration rate due to Coulomb interactions between Maxwellian particle distributions summed over ions and electrons and is given by

$$\nu_e^{\alpha/\beta} = 1.8 \times 10^{-19} \frac{\left(m_\alpha m_\beta\right)^{1/2} Z_\alpha^2 Z_\beta^2 n_\beta \lambda_{\alpha\beta}}{\left(m_\alpha T_\beta + m_\beta T_\alpha\right)^{3/2}} \mathrm{sec}^{-1} \tag{6}$$

where $\lambda_{\alpha\beta} \sim 10-20$ is the Coulomb logarithm [*Book*, 1990], and Z is the charge number. Note that the last term in equation (5), thermal equilibration, may be positive or negative, but we have included it in the source expression for simplicity. In the case of ionization or charge exchange involving neutrals, the input temperature is determined from the pickup energy given by

$$\frac{3}{2} T_{pu} = \frac{1}{2} m_\alpha v_{rel}^2 \tag{7}$$

where

$$v_{rel} = \Omega_J r - \left(\frac{GM_J}{r}\right)^{1/2} \tag{8}$$

is the relative velocity of corotating plasma with respect to the local Keplerian velocity.

[15] Similarly the energy loss for a given species is

$$\mathcal{L}_\mathcal{E} = I_\alpha n_e n_\alpha T_\alpha + I^h_\alpha n_{e,hot} n_\alpha T_\alpha + R_\alpha n_\alpha n_e T_\alpha + \sum_{\alpha,\beta} k_{\alpha,\beta} n_\alpha n_\beta T_\alpha + \frac{n_\alpha T_\alpha}{\tau} \tag{9}$$

The thermal electron temperature is determined by balance between energy gain by Coulomb collisions with ions, energy loss by radiation, and transport loss, so

$$\frac{\partial(n_e T_e)}{\partial t} = \sum_\beta \nu^{\beta/e} n_e \left(T_\beta - T_e\right) - \frac{2}{3} \sum_{\beta,\lambda} \rho_{\beta,\lambda} n_e n_\beta - \frac{n_e T_e}{\tau} \tag{10}$$

where $\rho_{\beta,\lambda}$ are the radiative rate coefficients given in Figure 2. The factor of 2/3 is necessary since the radiative rate coefficients are given in units of energy.

[16] The two sets of equations, (1) and (2), are solved iteratively using a modified Euler method with second order accuracy. Steady state solutions were independently verified using Newton's method for steady problems.

Table 1. Charge Exchange Reactions, L = 6.0, k_0 [*Smith and Strobel*, 1985], k_1-k_{16} [*McGrath and Johnson*, 1989]

Reaction	k, $\mathrm{cm^3 s^{-1}}$
$S^+ + S^{++} \rightarrow S^{+++} + S^+$	$k_0 = 8.1 \times 10^{-9}$
$S + S^+ \rightarrow S^+ + S$	$k_1 = 2.4 \times 10^{-8}$
$S + S^{++} \rightarrow S^+ + S^+$	$k_2 = 3 \times 10^{-10}$
$S + S^{++} \rightarrow S^{++} + S$	$k_3 = 7.8 \times 10^{-9}$
$S + S^{+++} \rightarrow S^+ + S^{++}$	$k_4 = 1.32 \times 10^{-8}$
$O + O^+ \rightarrow O^+ + O$	$k_5 = 1.32 \times 10^{-8}$
$O + O^{++} \rightarrow O^+ + O^+$	$k_6 = 5.2 \times 10^{-10}$
$O + O^{++} \rightarrow O^{++} + O$	$k_7 = 5.4 \times 10^{-9}$
$O + S^+ \rightarrow O^+ + S$	$k_8 = 6 \times 10^{-11}$
$S + O^+ \rightarrow S^+ + O$	$k_9 = 3.1 \times 10^{-9}$
$S + O^{++} \rightarrow S^+ + O^+$	$k_{10} = 2.34 \times 10^{-8}$
$S + O^{++} \rightarrow S^{++} + O^+ + e^-$	$k_{11} = 1.62 \times 10^{-8}$
$O + S^{++} \rightarrow O^+ + S^+$	$k_{12} = 2.3 \times 10^{-9}$
$O^{++} + S^+ \rightarrow O^+ + S^{++}$	$k_{13} = 1.4 \times 10^{-9}$
$O + S^{+++} \rightarrow O^+ + S^{++}$	$k_{14} = 1.92 \times 10^{-8}$
$O^{++} + S^{++} \rightarrow O^+ + S^{+++}$	$k_{15} = 9 \times 10^{-10}$
$S^{+++} + S^+ \rightarrow S^{++} + S^{++}$	$k_{16} = 3.6 \times 10^{-10}$

3.2. Velocity Distributions

[17] This analysis presupposes that the velocity distributions of each species can be approximated as Maxwellians for the purpose of calculating the energy transfer via Coulomb collisions. Such an approximation is probably

reasonable for the ions for which the thermal core to the velocity distribution seems to be an isotropic Maxwellian with about 15% of the ions in a suprathermal tail [*Crary et al.*, 1998; *Bagenal*, 1994]. Unless the source strength is high and/or the transport rate very low, the newly picked-up ions form a small fraction of the total ion population. *Frank and Paterson* [2001b, 2002] report detecting ~15% pickup ions near Io. As we discuss below, we estimate that only 2% of the total mass of the torus is added per 10-hour rotation period. Nevertheless, given that the transport loss and Coulomb collision timescales are comparable, the actual ion energy distributions may be better approximated by a thermal distribution plus a delta function at the pickup temperature. *Smith and Strobel* [1985] concluded that indeed the ion velocity distributions are significantly non-Maxwellian for the major species, with high-energy tails extending to the pickup energy. At the same time, the *Smith and Strobel* [1985] analysis underestimated the UV emission rates (specifically for S^+ ions) and the atomic data have been updated in the meantime [*Shemansky*, 1988].

[18] The velocity distribution of the electrons is critical as the electron energy affects the ionization and radiation rates as well as Coulomb coupling. To approximate the non-thermal electron distribution function and to regulate the additional source of heat needed to power the torus [*Shemansky*, 1988] we stipulate a fixed fraction of hot electrons (f_{eh}) with a fixed temperature (T_{eh}). Preliminary analysis of the Galileo electron energy distributions [*Frank and Paterson*, 2000a] and the Cassini UVIS [*Steffl*, 2002] spectra suggests that additional electron components at intermediate energies (or a κ-function) better approximate the non-thermal electron distribution function. In future studies we will explore the need to add further components to the electron distribution.

3.3. Torus Volume

[19] The primary source for the torus is the ionization of the extended neutral clouds sputtered from Io's atmosphere. To convert the volumetric source strength to a net source we need to know the volume of the source. The source is probably spatially inhomogeneous. Galileo observations and modeling dictate that where flow is stagnated very close to Io (2.4 R_{Io}) the Io interaction provides only ~20% of the source [*Bagenal et al.*, 1997; J. Saur, D. R. Strobel, F. M. Neubauer, and M. E. Summers, The ion mass loading rate at Io, manuscript submitted to *Journal of Geophysical Research*, 2002]. The extended neutral clouds are responsible for the remaining mass input, but the distributions of the extended neutral clouds are not well determined. Transport processes may also change the emitting volume. Nevertheless, for both net source and emission rates we take a torus volume of $2\pi 6\ R_J \times 1\ R_J^2 = 1.4 \times 10^{31}\ cm^3 = 38\ R_J^3$. If the source is confined to a smaller region then the net production determined by the model will be correspondingly less and if the emission volume is larger then the total emitted power predicted by the model will be correspondingly greater.

4. Results

4.1. Summary of Preliminary Voyager Era Results

[20] To compare our model with previous models [e.g., *Shemansky*, 1988; *Barbosa*, 1994; *Schreier et al.*, 1998], we have conducted a sensitivity study in a region of parameter space used in these previous models. Previous models used the Voyager 1 era composition as a benchmark and hence we label this region as the nominal Voyager case. Different regions of parameter space were also found to yield nominal Voyager results by *Lichtenberg and Thomas* [2001] and we will address this in an "extended exploration" below.

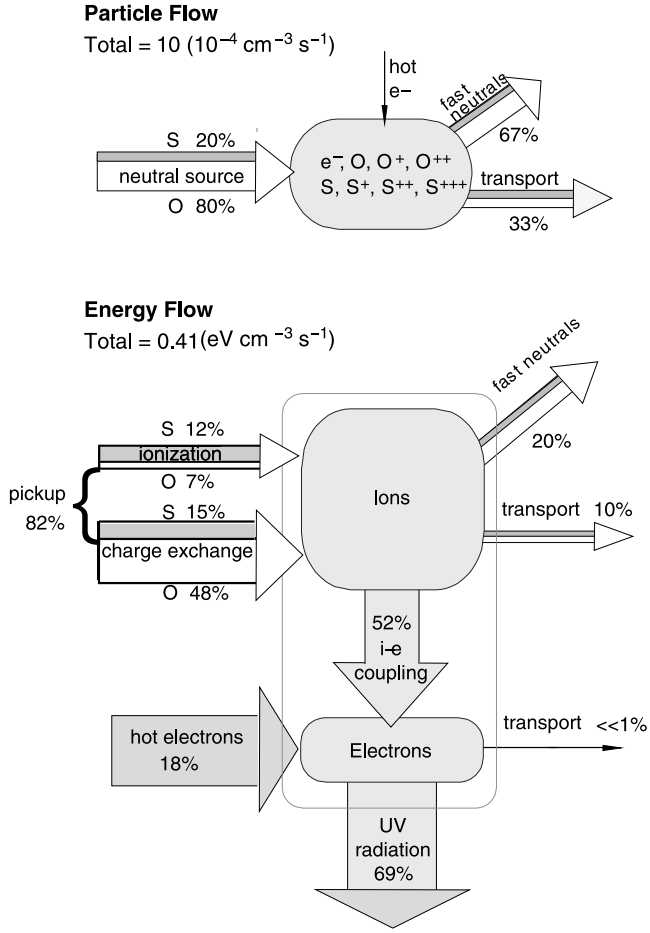

Figure 5. Mass and energy flow for "nominal" torus parameters (see Table 2). Mass flow units are 10^{-4} cm^{-3} s^{-1}, and energy flow units are in eV cm^{-3} s^{-1}.

[21] Figure 5 shows the mass and energy flow for nominal Voyager parameters (O/S = 4.0, τ = 50 days, $\mathcal{S}_n$ = 10 in units of (10^{-4} cm^{-3} s^{-1}), f_{eh} = 0.23%, and T_{eh} = 600 eV). For the nominal Voyager model parameters and assuming a torus source volume of 1.4×10^{31} cm^3 the net mass input rate is roughly 0.45 tons/s. Mass is lost from the system through fast neutral escape due to charge exchange involving pickup ions (67%) and from radial transport (33%) which ultimately leads to loss through the magnetotail. Energy is added to the torus through the energization of ionized material in the corotational electric field. Ionized material gains both corotational $\mathbf{v} \times \mathbf{B}$ drift as well as a gyration velocity equal to the local corotation velocity. Thus the ionization of neutral material (either via electron impact ionization or charge exchange of an ion with a neutral) is a primary energy source. Another significant and sometimes dominant source of energy is the thermal coupling between a small hot

electron population and the thermal core of the electrons. Energy flows from the hotter ion population to the thermal electron core which then radiates most of the energy away in the UV. Multiplying the volumetric emission rate of 69% of 0.4 eV cm^{-3} s^{-1} by the total torus volume of 1.4×10^{31} cm^3 produces a net emission power of 0.7×10^{12} W. (We discuss below possible explanations for why this is lower than usual Voyager 1 values of $2-3 \times 10^{12}$ W.) Transport and fast neutral escape are two less significant energy sinks.

[22] An example of a preliminary parameter space search from the NCT model is shown in Figure 6 which shows the sensitivity of torus composition to transport time (τ = 15–60 days) and neutral source rate ($\mathcal{S}_n = 4-20 \times 10^{-4}$ cm^{-3} s^{-1}) for a fixed a hot electron fraction (f_{eh} = 0.23%), hot electron temperature (T_{eh} = 600 eV), and O/S source ratios (O/S = 4.0). The 20 panels, ordered left to right and top to bottom, show: 1–2) neutral S and O density, 3) electron density, 4–8) ion mixing ratios, 9–10) S ion ratios, 11) average charge state, 12) ion abundance ratio, 13) electron temperature, 14) ion temperature, 15) ionization to charge exchange power input ratio, 16) fast neutral power sink, 17) transport power sink, 18) ion-to-electron thermal coupling, 19) UV power radiated, and 20) hot electron power input. The measured range of Voyager 1 conditions are shown by the shaded regions and the boxed regions indicate our choice for the best fit. The dashed line in the upper right corner indicates a region of non-equilibrium solutions where the strong source dominates transport losses which leads to a steady increase in plasma density. The electron density and ion temperature are from *Bagenal* [1994] and the range in ion composition comes from *Shemansky* [1988] and *Herbert et al.* [2000]. While we did not exhaustively explore the entire five-dimensional parameter space, we were not able to find a region that simultaneously matched all of the reported Voyager 1 conditions. For example, if we assume transport times of 40–50 days and source rates of $8-12 \times 10^{-4}$ cm^{-3} s^{-1}, we can match most of the conditions.

[23] Note that a total ionization source rate of $4-12 \times 10^{-4}$ cm^{-3} s^{-1} is consistent with net plasma production of $0.6-1.7 \times 10^{28}$ ions s^{-1} or 200–600 kg s^{-1} (O/S = 2.0) for a source volume of 38 R_J^3. Dividing a typical local electron density of 2000 cm^{-3} by the total source strength of 10×10^{-4} cm^{-3} s^{-1} gives a timescale for replenishment of the torus of 19 days. Equivalently, in a 10-hour jovian rotation period, only 2% of the torus is replenished.

4.1.1. Composition

[24] The model values of neutral densities, shown in Panels 1 and 2 ($n_O \sim 50-100$ cm^{-3}, $n_S \sim 5-10$ cm^{-3}), are consistent with observations of the extended neutral clouds [*Durrance et al.*, 1983; *Brown*, 1981; *Thomas*, 1996]. However, the observed composition (shaded regions in Panels 3–10) requires that the ratio of oxygen to sulfur neutral sources be greater than the expected value of 2 that would result from complete dissociation of SO_2. Mainly because of the efficiency of the $O + O^+ \rightarrow O^+ + O^*$ charge exchange reaction, oxygen neutrals are preferentially removed from the system and a source strength ratio O/S ~3 to 5 is needed to produce an ion composition that is consistent with Voyager era measurements.

[25] Locating the best fit to the Voyager 1 era conditions in the five-dimensional parameter space is made particularly difficult by the sensitivity of sulfur ion composition to small variations in a number of the input parameters. Oxygen ion composition is generally less sensitive to variations in input parameters (other than O/S ratio). The S^{++} mixing ratio remains roughly constant in the τ vs. $\mathcal{S}_n$ plane (Panel 5). The production of S^{++} is dominated by electron impact ionization of S^+ and by charge exchange between O and S^{+++} (k_{14}, Table 1). Thus as the relative abundance of S^+ decreases with increasing τ and $\mathcal{S}_n$, the production of S^{++} is compensated by an increasing relative abundance of S^{+++}. The primary difficulty in obtaining a best fit to Voyager 1 measurements was in matching the sulfur ion ratios (S^+/S^{++} and S^{+++}/S^{++}, Panels 9 and 10). We note, however, that charge exchange reaction k_{14} reported in *McGrath and Johnson* [1989] is one order of magnitude larger than the value reported by *Johnson and Strobel* [1982] and that *Shemansky* [1988] used the earlier, lower value to fit the measured Voyager 1 sulfur ion ratios. Reaction k_{14} is also responsible for roughly 85% of the S^{+++} loss in our model and therefore strongly affects the sulfur ion ratios.

[26] Panels 11 and 12 show the ion abundance ratio ($\Sigma O^+/\Sigma S^+$) and the average charge state ($n_e/\Sigma n_i$). The oxygen/sulfur abundance ratio is relatively insensitive to variations in transport time (τ) and neutral source rate ($\mathcal{S}_n$) and the nominal value of 1.35 is consistent with observations in the range 0.8 to 1.8 [*Shemansky*, 1988; *Herbert and Sandel*, 1995; *Bagenal*, 1994]. The average charge state (Panel 12), on the other hand, shows more sensitivity to variations in τ and $\mathcal{S}_n$, increasing for both increasing τ and increasing $\mathcal{S}_n$. The average charge state is expected to increase with τ and $\mathcal{S}_n$ as equilibrium will settle into the higher ionization states for longer plasma residence time.

4.1.2. Energy Flow

[27] The neutral clouds of S and O are ionized by electron impact ionization and ion/neutral charge exchange reactions. Sulfur is a factor of two more readily ionized by electrons than oxygen while oxygen is more readily ionized through charge exchange. Major problems in the construction of NCT models arise from changes in published values for the electron impact ionization rate coefficients for different ions as a function of electron temperature, particularly at lower energies (discussed in *Lichtenberg and Thomas* [2001]). The addition of small quantities of suprathermal electrons enhances the ionization rate, particularly to higher ionization states. When ionized, the fresh ion picks up gyromotion at the local flow speed resulting in corotational pickup energies for sulfur and oxygen ions of 540 eV and 270 eV respectively (~82% of power to the torus for nominal Voyager conditions). Note that the electron impact ionization of neutral S and O supplies only ~19% of total power input to the torus (~0.4 eV cm^{-3} s^{-1} or 9.0×10^{11} W) for the Voyager era. Charge exchange reactions do not change the total charge density, but they have major effects on composition as well as providing (through pick up of fresh ions) ~63% of the power to the torus. Pickup ions cool through thermal coupling with the core electron population, resulting in nominal electron and ion temperatures of roughly 5 eV and 100 eV respectively (Panels 13 and 14).

[28] Panel 15 shows the power input ratio of ionization compared to charge exchange. Throughout the nominal range of Voyager 1 parameters shown in Figure 6, charge

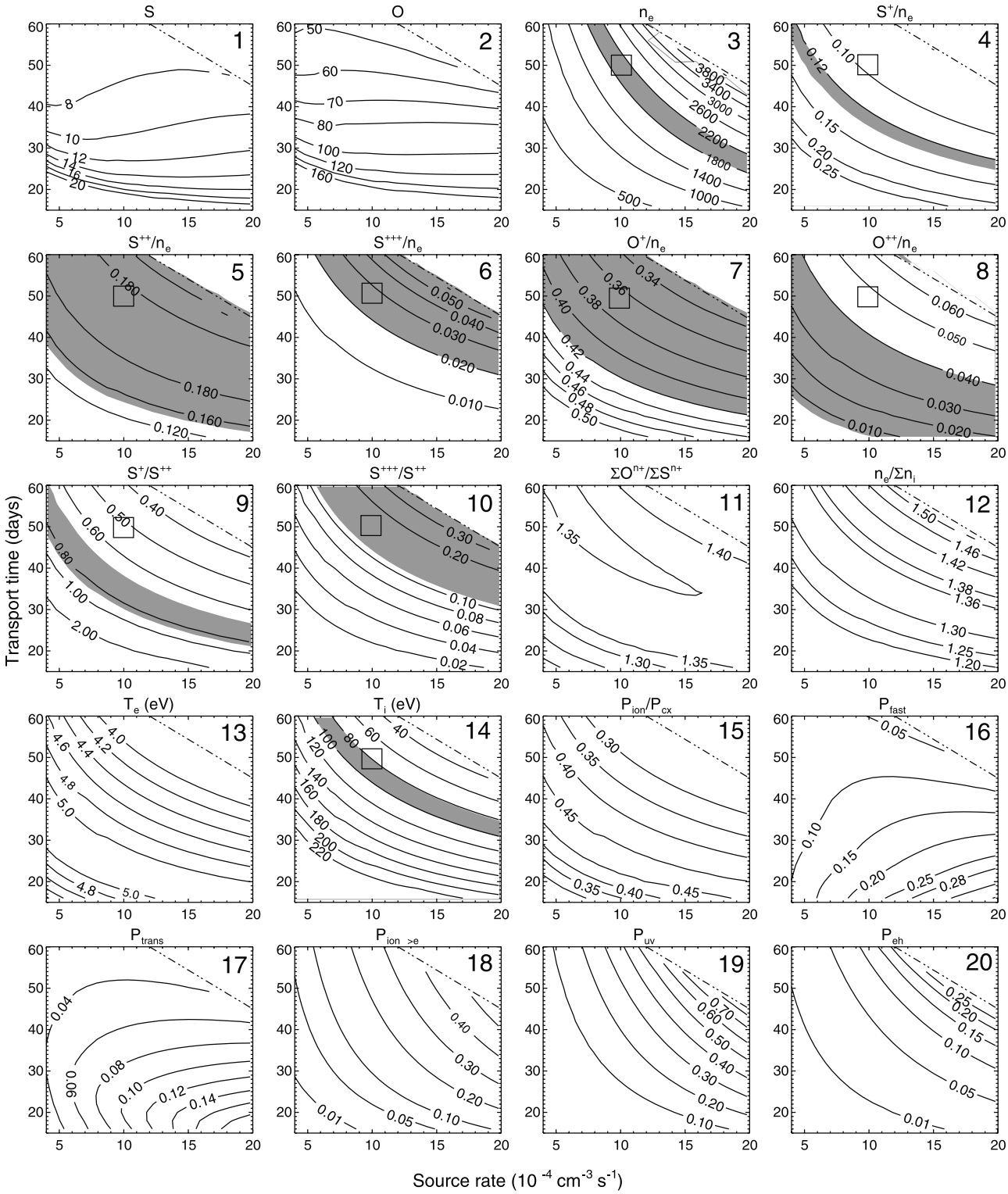

Figure 6. Nominal Voyager 1 era (f_{eh} = 0.23%, T_{eh} = 600 eV, O/S = 4.0). The shaded regions indicate the range of measured Voyager 1 era parameters. Our best fit to input parameters is shown by the boxed regions (τ = 50 days, $\mathcal{S}_n = 10 \times 10^{-4}$ cm^{-3} s^{-1}). Density is given in units of cm^{-3} and power is given in units of eV cm^{-3} s^{-1}.

exchange is the dominant source of pickup energy, contributing between 60–70% with respect to electron impact ionization. This is largely due to the efficiency of the O + $O^+ \rightarrow O^+ + O^*$ charge exchange reaction and the large O/S neutral source ratio (4.0) required for the best fit to the measured range of Voyager 1 era parameters. As will be discussed below, the Cassini era best fit uses a smaller O/S neutral source ratio of 1.7 and hence the hot electrons

provide the dominant energy input source (~60%) in the Cassini era.

[29] Neutralized ions maintain their velocity but are no longer confined by the magnetic field and rapidly leave the torus as fast neutrals at a volumetric rate of 6.7×10^{-4} cm^{-3} s^{-1}, or 9.4×10^{27} s^{-1} for a torus volume of 38 R_J^3. These fast neutrals carry away about 67% of the mass input but only 20% of the energy. Panel 16 shows the variations in power output through fast neutral escape. *Smyth* [1998] and *Smyth and Marconi* [2000] estimates 1.72×10^{28} neutral O and S atoms are removed from Io per second, 2/3 of which are lost to charge exchange, or 1.03×10^{28} s^{-1}. The [*Brown*, 1994] mass loading rate of $2-6 \times 10^{28}$ s^{-1} (or 640–2000 kg s^{-1}), derived from the few percent deviation of torus plasma from corotation, is consistent with model values for pick up from ionization and charge exchanged combined.

[30] Radial transport of plasma out of the torus is usually simplified in NCT models to a loss timescale $\tau \sim 8$ to 80 days, though most (Voyager era) models are converging on a rate of 40–60 days. For our nominal Voyager 1 conditions, radial transport of plasma removes 33% of the initial neutral mass but only 10% of the torus power. Panel 17 shows the power losses due to transport which interestingly is a function of both transport time and source strength. For large transport time, P_{trans} is weakly dependent on the source strength while for short transport time P_{trans} is strongly dependent on the source strength. The dependence on transport time is expected, but for sufficiently rapid transport the only way to increase P_{trans} is to add more material to the system with an increased neutral source rate.

[31] The energy picked up by a fresh ion is transferred by Coulomb collisions to electrons (at a nominal rate of 0.17 eV cm^{-3} s^{-1}, Panel 18). This ion cooling timescale is ~20 days (i.e., comparable to the transport timescale). The electrons quickly lose energy through excitation of the ions (which promptly radiate the energy, mostly at EUV wavelengths). The EUV emissions radiated by the torus add up to about 0.28 eV cm^{-3} s^{-1} which is about 69% of the total torus power throughput (Panel 19). Summing over a volume of ~38 R_J^3 we get a total emitted power of 0.6×10^{12} W. The values reported for Voyager 1 are $2-3 \times 10^{12}$ W (e.g., [*Strobel*, 1989]). Note that a comparison of total emitted power with the homogeneous model output is subject to an assumed total volume and to density inhomogeniety within the torus volume (e.g., emission is proportional to n_e^2 so a smaller volume of higher density in the core of the torus would lead to higher total emission).

[32] To produce this power it was pointed out by *Shemansky* [1988] that pickup energy is not sufficient and that an additional source of energy is needed. Several authors have investigated the efficacy of different potential sources of energy [*Smith and Strobel*, 1985; *Barbosa*, 1994; *Schreier et al.*, 1998] but there is a growing consensus that a small fraction of suprathermal electrons can readily supply the necessary additional 20% of the total power (see Panel 20). *Schreier et al.* [1998] make the point that the most efficient coupling would occur should the suprathermal electrons have a temperature about five times that of the thermal electrons (i.e., about 20–30 eV). Voyager in situ electron measurements indicate a small (1–2%) fraction of ~500 eV electrons [*Sittler and Strobel*, 1987]. We have varied the temperature and charge fraction of the hot electrons in the model to adjust the total power output (sensitive to electrons in the 5–30 eV range for EUV emissions) and to match observed fractions of ionization states.

4.2. Sensitivity Study (f_{eh}, T_{eh}, O/S)

[33] For a nominal transport time (τ = 50 days) and neutral source rate (10×10^{-4} cm^{-3} s^{-1}), sensitivity to: 1) the hot electron fraction, 2) hot electron temperature, and 3) the O/S source ratio can be investigated (cases 1,2,3 in Figure 7). Variations in the O/S source ratio, not surprisingly, change the mixing ratios in accordance with the relative abundance of the neutral O and S source. The total ion abundance ratio ($\Sigma O^{n+}/\Sigma S^{n+}$) varies between ~1.2 and 1.7 for O/S ranging from 3.0 to 5.0. In our nominal case of O/S = 4.0, $\Sigma O^{n+}/\Sigma S^{n+} \sim 1.4$. The average charge state shows very weak dependence to variations of any of these parameters with $n_e/\Sigma n_i \sim 1.4$.

[34] Changing the hot electron fraction (cases 1, 4, 5) strongly affects the S^+ and S^{++} mixing ratios and the ion temperatures while other variables show weak dependence. In particular, for f_{eh} varying between 0.35% and 0.15% the S^+ mixing ratio varies between 0.03 and 0.15 and the electron density varies between 3200 cm^{-3} and 1500 cm^{-3}. The average ion temperature increases from 30 eV to 100 eV and is anticorrelated with the electron density. The ions are thermally coupled to the electron population which radiates more efficiently at higher density, thus a decrease in electron density results in a dramatic increase in average ion temperature and only a slight increase in the electron temperature.

[35] Although ionization rates are weakly dependent on electron temperatures above 50 eV (Figure 3), variations in the hot electron temperature (cases 1, 6, 7) can significantly alter torus composition due to the temperature dependence of thermal coupling between hot and cold electrons and due to variations in the relative rate differences for a given pair of species as a function of temperature. The latter case is particularly important for the higher ionization states where hot electrons can play a dominant role in ion production and loss. For example, Figure 3 shows that the relative spacing between the ionization rates for S^+ and S^{++} decreases considerably above 50 eV. Although oxygen mixing ratios are fairly insensitive to the hot electron temperature, sulfur shows considerable sensitivity. For instance, the S^+ mixing ratio increases by a factor of two when T_{eh} is increased from 50 eV to 1000 eV while the O^{++} mixing ratio only increases by roughly 20%. The O^+, S^{++}, and S^{+++} mixing ratios all decrease slightly with increasing hot electron temperature. Surprisingly, the average charge state decreases slightly with increasing temperature. It is clear that with the added complexity of a strong dependence of torus composition on the hot electron temperature, a more exact specification of the energy distribution function will be crucial for future studies.

4.3. Extended Exploration

[36] *Lichtenberg and Thomas* [2001] found a best fit to the nominal Voyager composition in a very different region of parameter space as compared to previous NCT models.

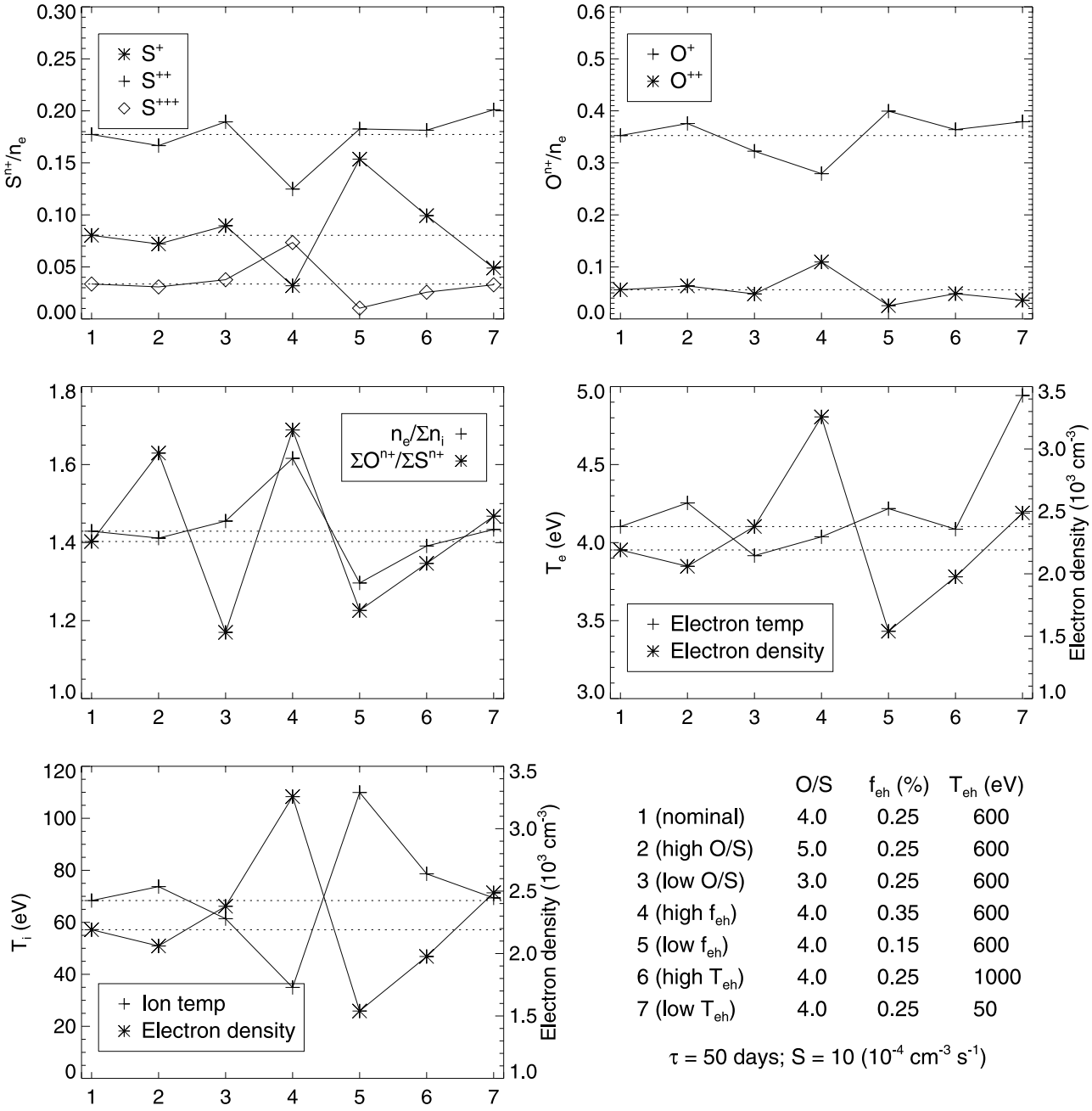

	O/S	f_{eh} (%)	T_{eh} (eV)
1 (nominal)	4.0	0.25	600
2 (high O/S)	5.0	0.25	600
3 (low O/S)	3.0	0.25	600
4 (high f_{eh})	4.0	0.35	600
5 (low f_{eh})	4.0	0.15	600
6 (high T_{eh})	4.0	0.25	1000
7 (low T_{eh})	4.0	0.25	50

Figure 7. Sensitivity of hot electron fraction (f_{eh}), hot electron temperature (T_{eh}), and O/S neutral source ration for fixed transport time (τ = 50 days), and neutral source rate ($\mathcal{S}_n = 10 \times 10^{-4}$ cm^{-3} s^{-1}). The parameters for seven cases are shown.

The *Lichtenberg and Thomas* [2001] solution used $\tau \sim$ 8 days, $\mathcal{S}_n \sim 50 \times 10^{-4}$ cm^{-3} s^{-1} and $f_{eh} = 0.5\%$ driven by the need to match ground-based measurements of S^{+++}. By conducting an extended exploration of the five-dimensional parameter space, we found that it is indeed possible to bridge the gap between the nominal Voyager case and the *Lichtenberg and Thomas* [2001] solution.

[37] Preliminary studies with our NCT model have demonstrated that equilibrium solutions can be found spanning a vast region of the five-dimensional parameter space. While a comprehensive and detailed exploration of the parameter space may appear overwhelming, our preliminary calculations have illustrated inter-connectivity between certain parameters which may place additional constraints on the solution domain of the five-dimensional parameter space. For example, Figure 8 shows a slice through a three-dimensional space consisting of neutral source rate ($\mathcal{S}_n$), transport time (τ) and the hot electron fraction (f_{eh}). In this figure we show τ vs. $\mathcal{S}_n$ while f_{eh} (not shown) is varied linearly with $\mathcal{S}_n$ from 0.1% to 0.5%. The varied hot electron fraction was necessary to maintain a Voyager-like composition over the entire range of $\mathcal{S}_n$. For instance, a higher f_{eh} is necessary to populate the higher ionization states at low transport timescales. The solution domain is bounded (ap-

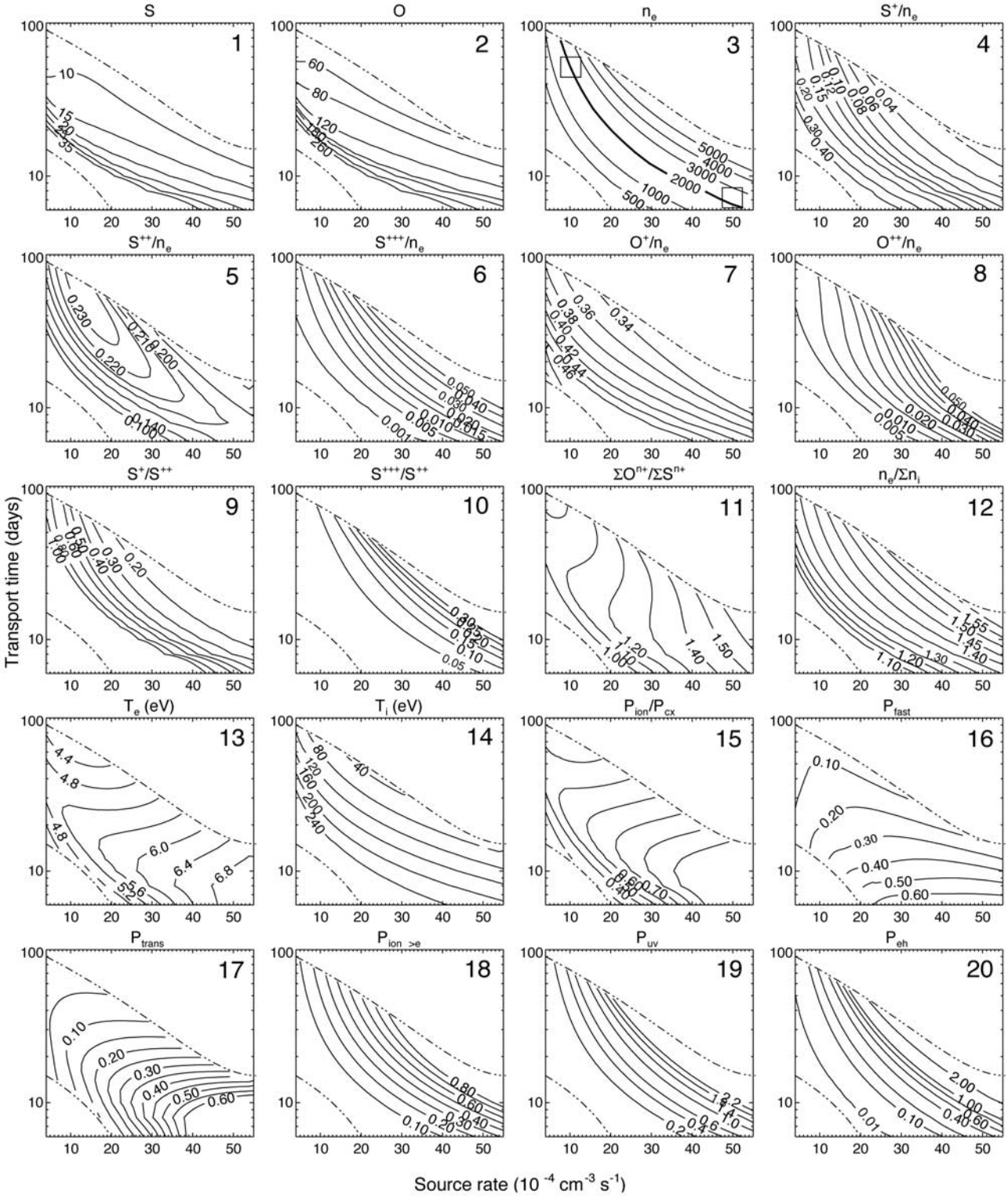

Figure 8. Extended exploration for transport time (τ = 6–80 days), neutral source rate ($\mathcal{S}_n$ = 4–55 × 10^{-4} cm^{-3} s^{-1}) and hot electron fraction (f_{eh} = 0.1–0.5%) for T_{eh} = 40 eV, and O/S = 3.0. The hot electron fraction is varied linearly with $\mathcal{S}_n$. The boxes in Panel 3 compare our nominal Voyager 1 best fit (upper left) with the *Lichtenberg and Thomas* [2001] solution (lower right).

proximately) from below by a mass-limited non-equilibrium region (due to rapid transport losses and minimal mass input), and above by a non-equilibrium energy-limited region (due to rapid cooling of the ions via thermal throughput to the electrons which efficiently radiate at high density).

[38] The contours shown in this slice through the three-dimensional space are consistent with the observed range of torus composition. In panel 3 the boxes illustrate our nominal Voyager 1 conditions (upper left) and the *Lichtenberg and Thomas* [2001] solution (lower right) which are connected by common contours. While the composition is roughly equivalent in these regions there are a number of important differences. The *Lichtenberg and Thomas* [2001] solution gives a higher thermal electron temperature (Panel 13), consistent with the efficient thermal coupling with a larger hot electron reservoir. The ion temperature is higher (200 eV, panel 14) as new pickup ions do not have sufficient time to transfer energy to the thermal electrons. With regard to energy input, pickup due to ionization dominates charge exchange (panel 15) and hot electron thermal coupling contributes significantly due to the increased hot electron fraction (panel 16). Energy losses through fast neutral escape increases due to the increasing abundance of neutral material (panels 1,2 and 17).

4.4. Voyager 2 and Cassini Results

[39] In addition to exploring the nominal Voyager 1 torus conditions, we provide model results for the Voyager 2 and Cassini era torus conditions (Figure 1). Figures 9 and 10 show sample parameter space searches. Again, the shaded regions indicate the measured values with ±10% range of uncertainty for Voyager 2 and measurement uncertainty for Cassini. In the case of Voyager 2 we found the best fit (boxed regions) for a high source rate ($\mathcal{S}_n \sim 30-40 \times 10^{-4}$ cm^{-3} s^{-1}), low transport time ($\tau \sim 18-25$ days), O/S = 4.0, T_{eh} = 600 (eV), and low hot electron fraction (f_{eh} = 0.12%). Again, we have had difficulty finding a location in parameter space consistent with all of the observations. In particular, we find the model predicts lower values for the S^{+++} ion fraction.

[40] Figure 10 shows a remarkably consistent fit to all observed conditions derived from Cassini UVIS in the top left corner of the plots with a low source strength and long transport time. Particularly useful in constraining the match is the total UV power emitted (P_{UV}) which has a much steeper curve in τ-$\mathcal{S}_n$ space than the composition curves. The best fit to Cassini values (boxed regions) was found to have a low source rate ($\mathcal{S}_n \sim 7 \times 10^{-4}$ cm^{-3} s^{-1}), high transport time ($\tau \sim 50$ days), O/S = 1.7, T_{eh} = 40 (eV), and f_{eh} = 0.3%. The P_{UV} constraint is based on a total emission of $2.0 \pm 0.5 \times 10^{12}$ W by an emitting volume of 1.4×10^{31} cm^3 to get a volumetric rates of 0.7–1.1 eV cm^{-3} s^{-1}. If we took a larger volume (e.g., 50%) then we would infer a lower volumetric emission of ~0.4 eV cm^{-3} s^{-1}. Note that the model can accommodate such a range in emitted power through a modest shift in source strength and still be consistent with the observed composition, but the model electron density correspondingly ranges from 1800 to 3000 cm^3. Little difficulty was encountered in fitting the sulfur ion ratios in the Cassini case. One possible explanation is that composition was less dependent on the potentially troublesome charge exchange reaction involving O and S^{+++} (k_{14}) due to the greater abundance of neutral sulfur relative to neutral oxygen (O/S = 1.7).

[41] Perhaps the most striking comparison of Voyager 1, Voyager 2, and Cassini cases is the variation in energy flow through the torus. Table 2 compares the energy throughput for the three separate cases based on the best fit from the respective parameter searches. Voyager 2 and Cassini are more extreme cases with Voyager 1 intermediate. Voyager 2 shows the highest throughput with 1.12×10^{-4} eV cm^{-3} s^{-1}, while Voyager 1 and Cassini are somewhat lower with 0.41 and 0.66×10^{-4} eV cm^{-3} s^{-1} respectively. The hot/cold electron thermal input varies significantly ranging from 11% for Voyager 2 to 60% for Cassini. As the power radiated increases along with the hot/cold electron thermal coupling input, the fast neutral losses and transport decrease.

5. Discussion

[42] We have used a neutral cloud theory model to explore a five-dimensional parameter space to gain insight in to the nature of torus variability. The parameter space is defined by the iogenic neutral source ($\mathcal{S}_n$), radial transport time (τ), neutral source O/S ratio (O/S), hot electron fraction (f_{eh}) and hot electron temperature (T_{eh}). Although there are many ways to explore the 5-D space, we elected to present variations in the neutral source strength and transport time for given O/S ratio, hot electron fraction and hot electron temperature. For plasma composition, a clear inverse relationship between transport time and source strength is present in all results. That is, for a given density and composition a wide range a solutions exist from large τ/small $\mathcal{S}_n$ to small τ/large $\mathcal{S}_n$. The goodness of fit can be tuned by adjusting the independent parameters, O/S, f_{eh}, and T_{eh}. The problem of uniqueness of solution is further compounded by the uncertainties in measurements and differences between torus compositions reported from analysis of the Voyager data sets. Thus the concept of nominal Voyager conditions should not be interpreted too rigorously. Nevertheless, there are distinctly different regions of parameter space that provide a "best fit" to the measured range of Voyager 1, Voyager 2, and Cassini era torus composition.

[43] The Voyager 1 era torus is perhaps best described by a 1 ton/s neutral source strength and a 50-day radial transport time, though given the wide range in measured composition one could argue for the case of large neutral source ($\mathcal{S}_n$ >2 tons/s) and small transport time (τ < 30 days). The limiting case for the Voyager 1 era would be the so-called "Lichtenberg solution" which requires a very large source strength of roughly 4 tons/s, a very short transport time of 8 days, and a larger hot electron fraction (~0.5% vs. 0.23%). Throughout the slice of parameter space shown in Figure 8 are plausible values for Voyager 1 era composition. It should be noted, however, that high source strengths and low transport times predict very high ion temperatures (>200 eV) which are inconsistent with Voyager plasma measurements [*Bagenal*, 1994]. Measurements of total UV power radiated and neutral density would provide particularly important constraints in locating a unique solution as these quantities contain an orthogonal component to the family of contours for plasma composition.

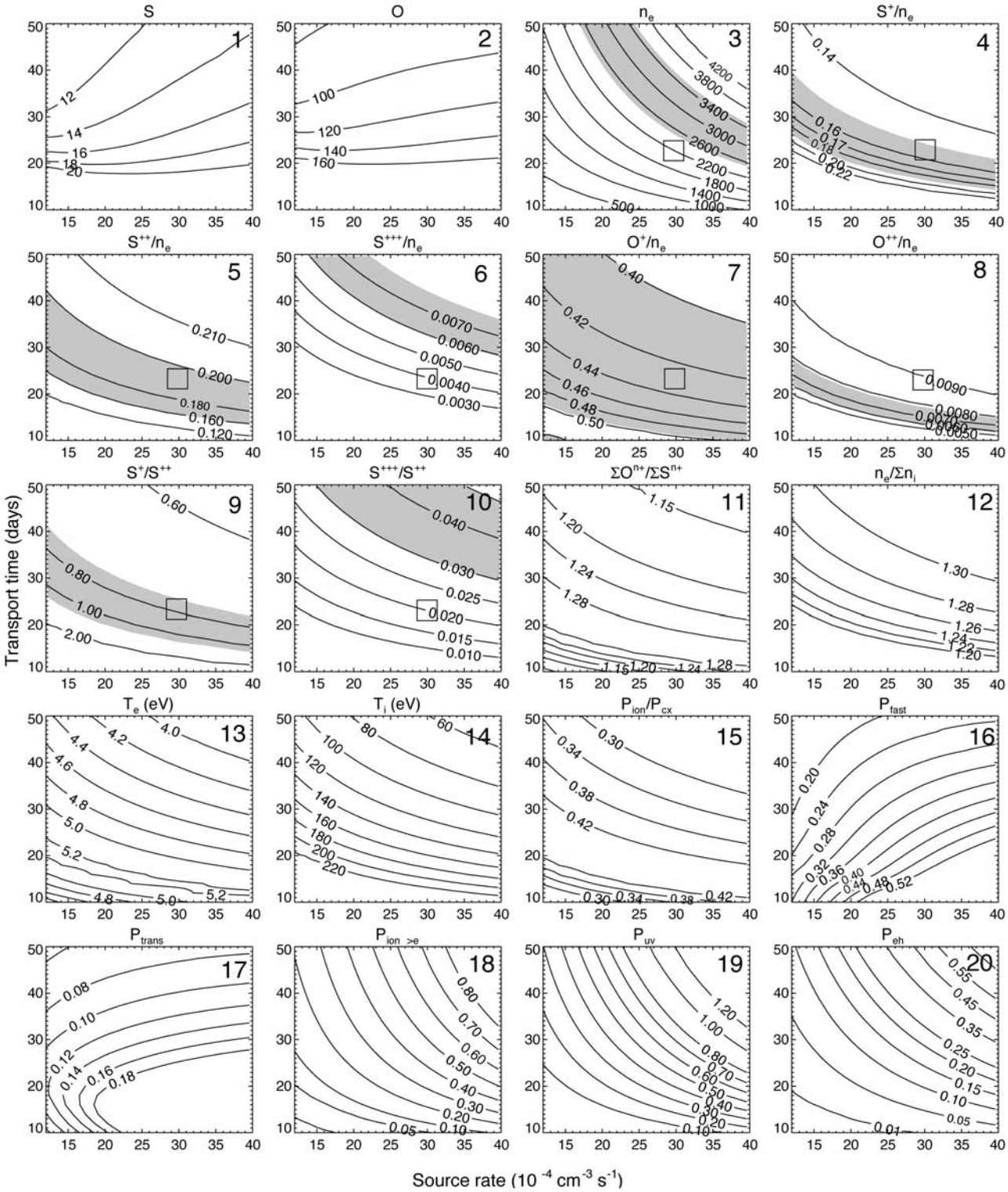

Figure 9. Nominal Voyager 2 era (f_{eh} = 0.12%, T_{eh} = 600 eV, O/S = 4.0). The shaded regions indicate measured Voyager 2 era parameters ±10%. Our best fit to input parameters is shown by the boxed regions (τ = 23 days, $\mathcal{S}_n = 30 \times 10^{-4}$ cm^{-3} s^{-1}).

[44] The Voyager 2 era torus is similar to Voyager 1 in that O/S source ratio of 4.0 for a "best fit" case is required. However, torus composition suggests that Voyager 2 may be best described with a high neutral source (~2.5 tons/s), a low transport time (~23 days) and a much smaller hot electron fraction (0.12%). Cassini, on the other hand, requires a much lower O/S ratio of 1.7 with a best fit for large τ (50 days) and small $\mathcal{S}_n$ (<1 ton/s). Despite the wide

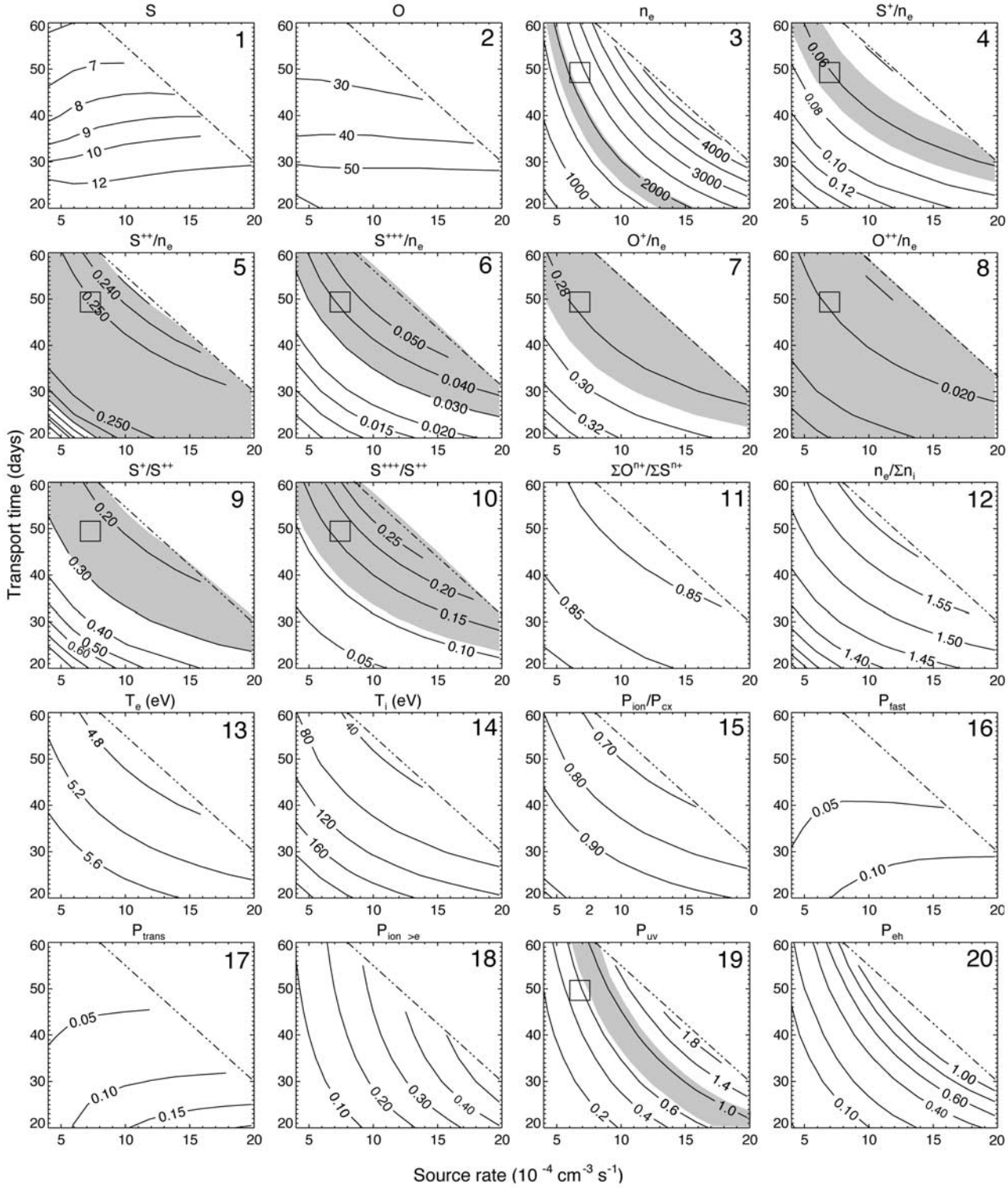

Figure 10. Nominal Cassini era (f_{eh} = 0.3%, T_{eh} = 40 eV, O/S = 1.7). The shaded regions indicate measured Cassini era values within experimental uncertainty. Our best fit to input parameters is shown by the boxed regions (τ = 50 days, $\mathcal{S}_n = 7 \times 10^{-4}$ cm^{-3} s^{-1}).

range of possible solutions, it is clear that Voyager 1, 2 and Cassini all favor very different regions of the five-dimensional parameter space, suggesting that indeed the torus composition is subject to very different conditions which are likely related to the Io's neutral source and volcanic activity. Particularly sensitive in the parameter search is the flow of energy through the torus. Table 2 illustrates the wide range of values for energy flow subject to different nominal input parameters. For instance, hot/cold electron thermal coupling ranges from 11% to 60% and the UV power

Table 2. Comparison of Energy Throughput for Nominal Voyager 1 (V1), Voyager 2 (V2), and Cassini Cases[a]

	V1	V2	Cassini
Nominal input parameters			
Neutral Source, $\mathcal{S}_n$ (10^{-4} cm^{-3} s^{-1})	10	30	7
Neutral Source O/S ratio	4.0	4.0	1.7
Neutral Source (tons/s)	0.80	2.40	0.64
Transport Time, τ (days)	50	23	50
Hot electron fraction, f_{eh} (%)	0.23	0.12	0.30
Hot electron temperature, T_{eh} (eV)	600	600	40
Energy flow (10^{-4} eV cm^{-3} s^{-1})			
Total power	0.41	1.12	0.66
Energy sources (%)			
S ionization	12	16	14
S charge exchange	15	13	8
O ionization	7	9	3
O charge exchange	48	51	15
Hot/cold electron thermal coupling	18	11	60
Internal thermal coupling (%)			
Ion-electron thermal coupling	52	32	29
Energy loses (%)			
Fast neutrals	20	40	5
Transport	10	18	6
UV radiation	69	42	89

[a]The neutral source in tons/s assumes an effective uniform torus volume of 2.5×10^{31} cm^3.

radiated ranges from 43% to 89% for Voyager 2 and Cassini respectively.

[45] Despite the apparent "hit or miss" nature of our parameter search, there are a few clear trends that emerge. First, for the modest range in observed plasma densities there is an inverse relationship between source strength and transport time. This is consistent with our expectations that increasing the source would lead to an initial enhancement in local density at Io's orbit. The increased density would then steepen the radial density gradient which likely increases radial transport through the gradient-driven flux tube interchange instability. Thus we postulate that there is a feedback loop between source and transport rates which results in a roughly constant plasma density in the torus. Second, the extended exploration shown in Figure 8 suggests that with an increased source and corresponding decreased transport time, the hot electron fraction must also increase. We postulate that the increased hot electrons arise from heating processes associated with the rapid radial transport.

[46] An obvious shortcoming of our model is the description of the hot electron population. This shortcoming is well illustrated by the relative importance of hot/cold electron thermal coupling. Thus an accurate description of the non-thermal electron tail is a crucial ingredient in torus composition and energy flow. The two-Maxwellian approximation adopted in our model for the electron population (cold core and hot tail) clearly does not adequately describe a more physically realistic κ-distribution [*Meyer-Vernet et al.*, 1995]. Future efforts will increase the number of parameters describing the hot electron population, adding another layer of complexity to the parameter search.

[47] In future studies we aim to explore the effects of adding more electron components to approximate a kappa distribution, find a systematic way of exploring multidimensional parameter space, and to model the time-variations in plasma conditions observed by the Cassini UVIS. Other issues to be considered include reconciling differences in published charge exchange reaction rates between O and S^{+++} (k_{14}), examining molecular sources (i.e., SO_2 and SO), describing variations in the neutral source spatial distribution (i.e., local and extended sources), and exploring Voyager temporal variations.

6. Conclusions

[48] Two decades of ground-based and space-based observations of the Io plasma torus suggest that the mass and energy flow through the torus can be highly variable. Neutral cloud models indicate that torus composition is consistent with roughly 1 ton/s escape of neutral material from Io which becomes ionized by electron impact ionization and charge exchange reactions. However, a comparison of the Voyager era and Cassini era torus composition suggests that Io's neutral source, both in total mass output as well as in composition, may vary significantly (Figure 1).

[49] A neutral cloud theory model has been developed to investigate the variability of mass and energy through the torus. The sensitivity of torus composition to nominal input parameters shows that despite a wide-ranging NCT model solution space coupled with experimental uncertainty (i.e., systematics in data analysis coupled with sensitivity to differences in the atomic emission rates and reaction rates used in the data analysis vs. model calculations) the best fits for Voyager 1, Voyager 2, and Cassini era torus conditions are in distinct regions of the five-dimensional parameter space. Thus we conclude that the torus is subject to considerable variability in the flow of mass and energy. The likely source of this variability in plasma conditions is changes in the iogenic neutral mass source which is responsible for generating neutral gas clouds in the form of a localized corona and extended clouds. Future improvements for this study include a better description of the non-thermal electron tail and a multidimensional (spatial) model to study radial, latitudinal, and longitudinal variations.

[50] The major findings of the paper are summarized below.

[51] 1. Torus conditions are distinctly different for the Voyager 1, 2 and Cassini era.

[52] 2. Unique torus input parameters for any given era are poorly constrained given the wide range of solution space that is consistent with the range of published torus conditions derived from different observations.

[53] 3. Ion composition is highly sensitive to the specification of a non-thermal electron distribution. While the range of parameter space that is consistent with observations at each epoch is quite large, the regions for each epoch are well separated. For example, the following parameter ranges are for the limiting cases of Cassini and Voyager 2 respectively.

[54] 4. Volumetric neutral source strengths: 7 to 30 $\times$ 10^{-4} cm^{-3} s^{-1} which corresponds to 0.4 to 1.3 tons/s for a volume of 38 R_J^3.

[55] 5. Neutral O/S source ratio: 1.7–4.0.

[56] 6. Transport times: 50–20 days.

[57] **Acknowledgments.** This study was supported by NASA award JPL959550 under the Galileo program.

[58] The Editor thanks Frank Crary and another reviewer for their assistance in evaluating this paper.

References

Bagenal, F., Empirical model of the Io plasma torus: Voyager measurements, *J. Geophys. Res.*, *99*, 11,043, 1994.

Bagenal, F., F. J. Crary, A. I. F. Stewart, N. M. Schneider, D. A. Gurnett, W. S. Kurth, L. A. Frank, and W. R. Paterson, Galileo measurements of plasma density in the Io torus, *Geophys. Res. Lett.*, *24*, 2119, 1997.

Barbosa, D. D., Neutral cloud theory of the Jovian nebula: Anomalous ionization effect of superthermal electrons, *Astrophys. J.*, *430*, 376, 1994.

Barbosa, D. D., and M. A. Moreno, A comprehensive model of ion diffusion and charge exchange in the cold Io torus, *J. Geophys. Res.*, *93*, 823, 1988.

Barbosa, D. D., F. V. Coroniti, and A. Eviatar, Coulomb thermal properties and stability of the Io plasma torus, *Astrophys. J.*, *274*, 429, 1983.

Book, D. L., *NRL Plasma Formulary*, Naval Res. Lab., Washington, D. C., 1990.

Broadfoot, A. L., Extreme ultraviolet observations from Voyager I encounter with Jupiter, *Science*, *204*, 979, 1979.

Brown, M. E., Observation of mass loading in the Io plasma torus, *Geophys. Res. Lett.*, *21*, 847, 1994.

Brown, R. A., The Jupiter hot plasma torus: Observed electron temperature and energy flows, *Astrophys. J.*, *244*, 1072, 1981.

Brown, R. A., C. B. Pilcher, and D. F. Stobel, Spectrophotometric studies of the Io torus, *Physics of the Jovian Magnetosphere*, pp. 197–225, Cambridge Univ. Press, New York, 1983.

Crary, F. J., F. Bagenal, L. A. Frank, and W. R. Paterson, Galileo plasma spectrometer measurements of composition and temperature in the Io plasma torus, *J. Geophys. Res.*, *103*, 29,359, 1998.

Dere, K. P., E. Landi, H. E. Mason, B. C. M. Fossi, and P. R. Young, CHIANTI-An atomic dataset for emission lines, *Astron. Astrophys. Supp.*, *125*, 149, 1997.

Dessler, A. J., (Ed.), *Physics of the Jovian Magnetosphere*, Cambridge Univ. Press, New York, 1983.

Durrance, S. T., P. D. Feldman, and H. A. Weaver, Rocket detection of ultraviolet emission from neutral oxygen and sulfur in the Io torus, *Astrophys. J.*, *267*, L125, 1983.

Esposito, L. W., et al., The Cassini ultraviolet imaging spectrograph investigation, *Space Sci. Rev.*, in press, 2003.

Feldman, P.-D., T. B. Ake, A. F. Berman, H. W. Moos, D. J. Sahnow, D. F. Strobel, H. A. Weaver, and P. R. Young, Detection of chlorine ions in the far ultraviolet spectrscopic explorer spectrum of the Io plasma torus, *Astrophys. J.*, *554*, L123, 2001.

Frank, L. A., and W. R. Paterson, Observations of plasmas in the Io torus with the Galileo spacecraft, *J. Geophys. Res.*, *105*, 16,017, 2000a.

Frank, L. A., and W. R. Paterson, Return to Io by the Galileo spacecraft: Plasma observations, *J. Geophys. Res.*, *105*, 25,363, 2000b.

Frank, L. A., and W. R. Paterson, Survey of thermal ions in the Io plasma torus with the Galileo spacecraft, *J. Geophys. Res.*, *106*, 6131, 2001a.

Frank, L. A., and W. R. Paterson, Passage through Io's ionospheric plasmas by the Galileo spacecraft, *J. Geophys. Res.*, *106*, 26,209, 2001b.

Frank, L. A., and W. R. Paterson, Plasmas observed with the Galileo spacecraft during its flyby over Io's northern polar region, *J. Geophys. Res.*, *107*(A12), 1478, doi:10.1029/2001JA009150, 2002.

Frank, L. A., W. R. Paterson, K. L. Ackerson, V. M. Vasyliunas, F. V. Coroniti, and S. L. Bolton, Plasma observations at Io with the Galileo spacecraft, *Nature*, *274*, 394, 1996.

Gurnett, D. A., W. S. Kurth, A. Roux, S. J. Bolton, and C. F. Kennel, Galileo plasma wave observations in the Io plasma torus and near Io, *Science*, *274*, 391, 1996.

Gurnett, D. A., A. Persoon, and W. Kurth, Electron densities near Io from Galileo plasma wave observations, *J. Geophys. Res.*, *106*, 26,225, 2001.

Herbert, F., and B. R. Sandel, Radial profiles of ion density and parallel temperature in the io plasma torus during the Voyager 1 encounter, *J. Geophys. Res.*, *100*, 19,513, 1995.

Herbert, F., et al., Azimuthal variation of ion density and electron temperature in the Io plasma torus, *J. Geophys. Res.*, *105*, 16,035–16,052, 2000.

Herbert, F., et al., Extreme Ultraviolet Explorer spectra of the Io plasma torus, *J. Geophys. Res.*, *106*, 26,293, 2001.

Herbert, F., et al., Hubble Space Telescope observations of sulfur ions in the Io plasma torus: New constraints on the plasma distribution, *J. Geophys. Res.*, *108*(A5), doi:10.1029/2002JA009510, 1167, 2003.

Johnson, R. E., and D. F. Strobel, Charge exchange in the Io torus and exosphere, *J. Geophys. Res.*, *87*, 10,385, 1982.

Lichtenberg, G., Massenbilanz und Energiehaushalt des Io-Plasma-Torus: Modell und Beobachtung, Ph.D. thesis, Univ. of Göttingen, Göttingen, Germany, 2001.

Lichtenberg, G., and N. Thomas, Detection of S (IV) 10.51 μm emission from the Io plasma torus, *J. Geophys. Res.*, *106*, 29,899, 2001.

Matheson, and D. E. Shemansky, 1993, unpublished manuscript.

Mazzotta, P., G. Mazzitelli, S. Colafrancesco, and N. Vittorio, Ionization balance for optically thin plasmas: Rate coefficients for all atoms and ions of the elements H to Ni, *Astron. Astrophys. Suppl. Ser.*, *133*, 403, 1998.

McGrath, M. A., and R. E. Johnson, Charge exchange cross sections for the Io plasma torus, *J. Geophys. Res.*, *94*, 2677, 1989.

McGrath, M. A., P. D. Feldman, D. F. Strobel, H. W. Moos, and G. E. Ballester, Detection of [oii] 2471 from the Io plasma torus, *Ap. J.*, *415*, 450, 1993.

Meyer-Vernet, N., M. Moncuquet, and S. Hoang, Temperature inversion in the Io plasma torus, *Icarus*, *116*, 202, 1995.

Moreno, M. A., and D. D. Barbosa, Mass and energy balance of the cold Io torus, *J. Geophys. Res.*, *91*, 8993, 1986.

Pequignot, D., P. Petitjean, and C. Boisson, Total and effective radiative recombination coefficients, *Astron. Astrophys.*, *251*, 680, 1991.

Richardson, J. D., and G. L. Siscoe, The problem of cooling the cold Io torus, *J. Geophys. Res.*, *88*, 2001, 1983.

Schreier, R., A. Eviatar, and V. M. Vasyliunas, A two-dimensional model of plasma transport and chemistry in the Jovian magnetosphere, *J. Geophys. Res.*, *103*, 19,901, 1998.

Shemansky, D. E., Ratio of oxygen to sulfur in the Io plasma torus, *J. Geophys. Res.*, *92*, 6141, 1987.

Shemansky, D. E., Energy branching in the Io plasma torus: The failure of neutral cloud theory, *J. Geophys. Res.*, *93*, 1773, 1988.

Shull, J. M., and M. V. Steenberg, The ionization equilibrium of astrophysically abundant elements, *Astrophys. J.*, *48*, 95, 1982.

Sittler, E. C., and D. F. Strobel, Io plasma torus electrons: Voyager 1, *J. Geophys. Res.*, *92*, 5741, 1987.

Smith, R. A., and D. F. Strobel, Energy partitioning in the Io plasma torus, *J. Geophys. Res.*, *90*, 9469, 1985.

Smyth, W. H., Neutral cloud distribution in the Jovian system, *Adv. Space. Res.*, *12*, 337, 1992.

Smyth, W. H., Energy escape rate of neutrals from Io and the implications for local magnetospheric interactions, *J. Geophys. Res.*, *103*, 11,941, 1998.

Smyth, W. H., and M. L. Marconi, Io's oxygen source: Determination from ground-based observations and implications for the plasma torus, *J. Geophys. Res.*, *105*, 7783, 2000.

Spencer, J. R., and N. M. Schneider, Io on the eve of the Galileo mission, *Annu. Rev. Earth Planet. Sci.*, *24*, 125–190, 1996.

Steffl, A., Cassini UVIS observations of the Io plasma torus, 2002, manuscript in preparation.

Stewart, I., UVIS observations at Jupiter, *Eos Trans. AGU*, *82*(17), Spring Meet. Suppl., 2001.

Strobel, D. F., Energetics, luminosity, and spectroscopy of Io's torus, *NASA Spec. Publ., NASA-SP-494*, 183, 1989.

Thomas, N., High resolution spectra of Io's neutral potasium and oxygen clouds, *Astron. Astrophys.*, *313*, 306, 1996.

Thomas, N., High resolution spectroscopy of the Io plasma torus, *J. Geophys. Res.*, *106*, 26,277, 2001.

Voronov, G. S., A practical fit formula for ionization rate coefficients of atoms and ions by electron impact: $Z = 1–28$, *At. Data Nucl. Data Tables*, *65*, 1, 1997.

Ziegler, D. L., J. H. Newman, L. N. Goeller, K. A. Smith, and R. F. Stebbings, Single and multiple ionization of sulfur atoms by electron impact ionization, *Planet. Space Sci.*, *30*, 1269, 1982.

F. Bagenal and P. A. Delamere, Laboratory for Atmospheric and Space Physics, University of Colorado, CB 392 Duane Physics, Boulder, CO 80309, USA. (bagenal@lasp.colorado.edu; delamere@lasp.colorado.edu)